Journal of Groundwater Science and Engineering
ISSN 2305-7068
Indexed by ESCI CABI CSA
Scopus GeoRef AJ CNKI

Evaluation of groundwater artificial recharge potential in the western Huaibei Plain, China

Pei-gui Liu, Ying-kang Yuan, Man-ting Shang, Zhi Li, Meng Liu

Citation:
Liu PG, Yuan YK, Shang MT, Li Z, Liu M. 2026. Evaluation of groundwater artificial recharge potential in the western Huaibei Plain, China. Journal of Groundwater Science and Engineering, 14(4): 535-554.

View online: https://doi.org/10.26599/JGSE.2026.9280093

Articles you may be interested in

Assessing the impact of artificial recharge on groundwater in an over-exploited aquifer: A case study in the Cheria Basin, North-East of Algeria
Journal of Groundwater Science and Engineering. 2023, 11(3): 263-277 https://doi.org/10.26599/JGSE.2023.9280022

Optimizing groundwater recharge plan in North China Plain to repair shallow groundwater depression zone, China
Journal of Groundwater Science and Engineering. 2023, 11(2): 133-145 https://doi.org/10.26599/JGSE.2023.9280012

Clogging mechanisms and preventive measures in artificial recharge systems
Journal of Groundwater Science and Engineering. 2021, 9(3): 181-201 https://doi.org/10.19637/j.cnki.2305-7068.2021.03.002

Quantifying groundwater recharge and discharge for the middle reach of Heihe River of China using isotope mass balance method
Journal of Groundwater Science and Engineering. 2021, 9(3): 225-232 https://doi.org/10.19637/j.cnki.2305-7068.2021.03.005

Effective groundwater level recovery from mining reduction: Case study of Baoding and Shijiazhuang Plain area
Journal of Groundwater Science and Engineering. 2023, 11(3): 278-293 https://doi.org/10.26599/JGSE.2023.9280023

Assessment of water level threshold for groundwater restoration and over-exploitation remediation the Beijing-Tianjin-Hebei Plain
Journal of Groundwater Science and Engineering. 2022, 10(2): 113-127 https://doi.org/10.19637/j.cnki.2305-7068.2022.02.002

Journal homepage: http://gwse.iheg.org.cn

Research Article

Evaluation of groundwater artificial recharge potential in the western Huaibei Plain, China

Pei-gui Liu[1*], Ying-kang Yuan[1], Man-ting Shang[1], Zhi Li[1], Meng Liu[2]

[1] *School of Civil Engineering*, *Hefei University of Technology*, *Hefei* 230009, *China*.
[2] *Anhui and Huaihe River Institute of Hydraulic Research*, *Hefei* 230088, *China*.

Abstract: To mitigate groundwater overexploitation and support the scientifically informed siting of artificial recharge infrastructure in the western Huaibei Plain, this study develops a multi-criteria evaluation framework for recharge suitability, focusing on the western portion of the Huaibei Plain. The framework integrates five hydrogeologically significant indicators: Groundwater table depth, saturated thickness of the primary aquifer, hydraulic conductivity, precipitation infiltration coefficient, and proximity to perennial rivers. Indicator weights were determined through a hybrid weighting strategy—combining the analytic hierarchy process, criteria importance through intercriteria correlation, and coefficient of variation methods—to balance subjective judgment with objective data-driven variance. These weights were spatially implemented using ArcGIS-based multi-criteria decision analysis to generate a continuous recharge suitability index map. The integrated weights derived from the hybrid approach are 0.222, 0.254, 0.173, 0.185, and 0.166 for the respective indicators. Recharge suitability was classified into four ordinal categories—high, moderate, low, and unsuitable—using the natural breaks optimization method. High and moderate potential zones collectively occupy 32.93% of the study area and are predominantly located in Funan, Qiaocheng, Guoyang, and Mengcheng counties—regions identified as priority candidates for artificial recharge project implementation. A sensitivity analysis confirms the stability and reliability of the zoning outcomes under parameter perturbation. By quantitatively identifying dominant controlling factors, delineating spatially explicit potential classes, and pinpointing priority implementation zones, this study establishes a transferable methodological framework. It directly supports sustainable groundwater management in the western Huaibei Plain and offers actionable guidance for optimizing recharge infrastructure placement. Moreover, the approach demonstrates broad applicability for recharge potential assessment and integrated water resources planning in hydrologically similar alluvial plain settings.

Keywords: Groundwater artificial recharge; Potential level; Coupled method; Sensitivity analysis; Huaibei Plain

Received: 27 Jan 2025/ Accepted: 16 Apr 2026/ Published: 10 Oct 2026

Introduction

With rapid socioeconomic development, the scale of global groundwater exploitation has continued to expand. Unreasonable exploitation has triggered large-scale environmental geological problems such as land subsidence (Shahkarami, 2024). For example, groundwater over-exploitation in the Oum Errabia Basin of Morocco (Jamali et al., 2020) has caused problems including groundwater level decline and water quality deterioration. The Mekong Delta in Vietnam (Dörr et al., 2023) and the Houston area of Texas in the United States are facing severe land subsidence problems due to long-term over-exploitation of groundwater. To address the global environmental geological prob-

*Corresponding author: Pei-gui Liu, *E-mail address*: liupg2512@163.com

DOI: 10.26599/JGSE.2026.9280093

Liu PG, Yuan YK, Shang MT, et al. 2026. Evaluation of groundwater artificial recharge potential in the western Huaibei Plain, China. Journal of Groundwater Science and Engineering, 14(4): 535-554.

2305-7068/© 2026 Journal of Groundwater Science and Engineering Editorial Office This is an open access article under the CC BY-NC-ND license (http://creativecommons.org/licenses/by-nc-nd/4.0)

lems caused by groundwater over-exploitation and ensure the sustainable development and utilization of water resources to support economic and social development, it is imperative to implement groundwater management and protection in over-exploitation areas.

Artificial groundwater recharge is a commonly used engineering measure to control groundwater over-exploitation. It refers to the process of augmenting the infiltration and recharge of groundwater resources from water sources such as surface water, rainwater, and reclaimed water through specific water conservation engineering measures. This technology can be traced back to China in 221 BC, when people excavated channels to guide surface water infiltration to improve groundwater quality (Zhang et al., 2020). This technology has been systematically applied in arid and semi-arid plain regions around the world; for example, scholars have used the Non-dominated Sorting Genetic Algorithm II (NSGA-II) to optimize the impact of artificial recharge systems on water level fluctuations and pollutant concentration changes in the aquifer of the Shahr Plain, Iran (Salehi Shafa et al., 2023). Other researchers identified potential groundwater artificial recharge zones in the Temara Plain of Morocco using Geographic Information System (GIS) and the Analytic Hierarchy Process (AHP) (Kadiri et al., 2023). The Upper Friuli Plain in Italy selected the Meretodi Tomba area to assess the impacts resulting from Artificial Recharge (AR) (Martelli et al., 2014). Accurate identification of suitable recharge zones is the key step in groundwater artificial recharge (Zhang et al., 2020).

Currently, the primary methods for evaluating the suitability of artificial groundwater recharge include experimental methods, numerical simulation methods, single-index evaluation methods, and multi-index comprehensive evaluation methods. For instance, Mogaji et al. (2016) applied the EBF-DST (Evidence Belief Function model framework based on Dempster-Shafer theory) model based on data from pumping tests and other sources to identify suitable artificial recharge zones in the hard rock geological area of southwestern Nigeria. Zaidi et al. (2015) adopted Boolean logic in the GIS environment, integrated parameters such as slope and aquifer type, and delineated potential groundwater artificial recharge zones in northwestern Saudi Arabia. Arya et al. (2020) selected factors such as soil and groundwater level with the help of GIS and remote sensing technology to identify prospective groundwater development zones in the Vattamalaikarai River Basin in southern India. Mishra et al. (2023) proposed a groundwater recharge zone positioning method integrating electrical resistivity tomography, sediment characterization, and dynamic monitoring technology. Biswas et al. (2023) proposed the concept of possible intermediate value of an asymmetric linear pentagonal fuzzy number for site selection of groundwater artificial recharge projects in basalt terrain areas. The above suitability evaluation methods provide important references for the determination of recharge zone suitability. Among all methods, the multi-index comprehensive evaluation method is favoured by many researchers because it can comprehensively consider the impact of each evaluation index on the final evaluation result and has high evaluation accuracy.

The core of this method lies in selecting appropriate evaluation indicators and scientifically calculating the index weights. In terms of index selection, scholars including, Ajjur and Mogheir (2019), Rani et al. (2019) and Aju et al. (2021) all listed slope as one of the evaluation indicators. They argued that under stable conditions where rainfall intensity is much greater than saturated hydraulic conductivity, subsurface runoff decreases with increasing slope. Raja and Mathew (2023) combined GIS, Remote Sensing (RS) and Multi-Criteria Decision Making (MCDM) technologies, further integrating drainage density, distance to river and elevation in addition to slope, to construct an evaluation system adapted to local conditions, and identified suitable groundwater artificial recharge zones in the Mareddu Basin, India. The selection of these indicators is based on a combination of regional conditions and practical needs, considering both the universality and regional adaptability of the evaluation indicators.

In terms of the calculation of evaluation indicator weights, methods can be broadly categorised into subjective and objective. At the subjective level, the commonly used subjective weighting method is the Analytic Hierarchy Process (AHP). This method has a mature calculation system and is widely used, but it is mainly affected by the subjectivity of researchers and relevant evaluation experts. For example, Mengstie et al. (2024) used the Analytic Hierarchy Process in identifying landslide-prone areas, and Shahkarami et al. (2024) used it when establishing a coastal vulnerability index for low-lying areas. In the evaluation of suitability for artificial groundwater recharge, Agarwal and Garg (2016), Aloui et al. (2022), Kadiri et al. (2023), Dubey et al. (2024) and Subba Rao et al. (2022) all used the analytic hierarchy process to

calculate factor weights to determine suitable artificial recharge zones, and achieved good results. At the objective level, objective weighting methods such as the CRITIC method are highly objective and can fully reflect the discrimination ability and independent information contribution of indicators, but they mostly rely on data quality and are relatively complex to calculate. For example, Zhang (2020) constructed a GIS-EWM multi-index comprehensive evaluation model, calculated the weights of each indicator, and evaluated and zoned the suitability of artificial groundwater recharge in the plain area of the Daqing River Basin. Existing studies have adopted the coupled subjective-objective weighting method, and its advantage of reducing evaluation bias has been verified in the evaluation of the Shichuan River Basin (Fan et al., 2023). The objective weight calculated by the data-driven method is coupled with the subjective weight obtained by the analytic hierarchy process, which not only compensates for the empirical bias of subjective weighting, but also considers the actual variability and correlation of indicators. The application of the above multi-index evaluation methods in the field of groundwater artificial recharge provides important references for subsequent research.

The western part of the Huaibei Plain in China, as a key grain-producing area and densely populated region, has historically relied heavily on groundwater for urban living and agricultural irrigation. Over the decades, groundwater extraction has increased dramatically from 0.9 billion cubic meters in the 1970s to 3 billion cubic meters by the early 21st century. However, insufficient groundwater management, combined with excessive and unregulated exploitation, has triggered a range of severe environmental challenges. Fuyang City has witnessed maximum cumulative land subsidence of up to 1.6 m; regional groundwater depression cones have emerged in cities such as Bozhou, where water levels at cone centers have dropped to depths of 50–80 m. Historically influenced by repeated flood deposits from the Yellow River, the western Huaibei Plain exhibits a distinctive hydrogeological structure, characterized primarily by a shallow vadose zone composed of low-permeability Shajiang black soil. This lithological setting, combined with pronounced spatial heterogeneity in aquifer productivity, limits the applicability of conventional groundwater recharge assessment methods, which often fail to resolve site-specific hydrological complexities. In response to escalating geo-environmental challenges, including widespread land subsidence and progressive deterioration of groundwater quality attributable to long-term over-extraction, there is an urgent need for targeted, science-informed engineering interventions.

Moving beyond theoretical zoning, this study employs ArcGIS-based spatial analysis to translate recharge potential assessments into actionable, county-level spatial outputs (e.g., Funan and Qiaocheng Counties), thereby bridging the gap between regional-scale evaluation and site-specific implementation. By aligning rigorous hydrogeological evaluation with operational requirements of local water resource management, the study advances high-resolution artificial recharge zoning—a capability previously underdeveloped in the region. As such, it delivers a scientifically grounded, spatially explicit foundation for designing differentiated artificial recharge strategies that reflect the hydrogeological uniqueness of each subregion.

To address these challenges, this study establishes an adaptive evaluation system specifically tailored to the western Huaibei Plain, characterized by two primary methodological innovations. First, this study introduces a tri-hybrid coupled weighting strategy—integrating the Analytic Hierarchy Process (AHP), CRITIC, and the Coefficient of Variation (CV)—marking its first application in groundwater recharge potential assessment within this region. This synergy effectively harmonizes subjective hydrogeological expertise with objective data-driven variance, thereby mitigating the inherent biases of single-method approaches and ensuring a high degree of rationality in indicator allocation. Second, this research enhances the Morris Sensitivity Analysis by innovatively applying it to the weight-allocation phase. This advancement allows for the precise quantification of how fluctuations in indicator weights propagate through the spatial zoning outcomes. By identifying the dominant controlling factors and their impact on suitability, this study significantly bolsters the robustness and reliability of the evaluation conclusions. Ultimately, this study not only offers a solid scientific foundation for pinpointing optimal recharge zones but also provides a replicable and transferable theoretical paradigm for sustainable water resource management in similar alluvial plain settings globally.

1 Study area

1.1 Geographical conditions

The western part of the Huaibei Plain, which is

located in the middle reaches of the Huai River basin, includes the cities of Bozhou and Fuyang and covers an area of approximately 18,500 square kilometers (Fig. 1). The entire region is characterized by flat plain terrain. However, due to the interlacing sedimentation of ancient rivers and the erosion and deposition caused by the historical southward breaches of the Yellow River, the local ground is not entirely smooth. The overall topography is sloped, being higher in the northwest and lower in the southeast, with a ground gradient of between 1/7,500 and 1/10,000. The area has a warm, temperate, semi-humid climate, with an average annual temperature of 15°C–16°C and an average annual precipitation of about 900 mm. Major rivers within the study area include the Huai River, Guo River, Cihuaixin River, Ying River, and Xifei River.

1.2 Hydrogeology

The western part of the Huaibei Plain is entirely covered by Quaternary deposits, which from the bottom to the top can be divided into the Lower Pleistocene (Q_1), Middle Pleistocene (Q_2), Upper Pleistocene (Q_3), and Holocene (Q_4). The types of groundwater in the western part of the Huaibei Plain are relatively simple, with no significant presence of carbonate-rock-fracture-karst water-bearing rock groups, clastic-rock-pore-fracture water-bearing rock groups, or magmatic-rock-fracture water-bearing rock groups. The vast majority of groundwater is loose-rock pore water. Based on the hydrogeological characteristics and other conditions of the groundwater, aquifers can be divided into shallow, middle-deep, and deep groundwater.

The shallow aquifer group is primarily composed of the Upper Pleistocene and Holocene; this group is widely distributed throughout the region and buried within 50 m of the surface. It has a close connection with atmospheric precipitation and surface water. The aquifer sands of this group are fine-grained, mainly consisting of silt, with a loose structure and varying sand layer thickness. The thickness of the sand layers is controlled by ancient river channels; the sand layers are thicker in areas with ancient river channels and thinner between them. The middle-deep aquifer group is mainly composed of the middle Pleistocene and the lower Pleistocene of the Quaternary, with sand depths ranging from 50 m to 150 m and the groundwater confined. The sand layers that host

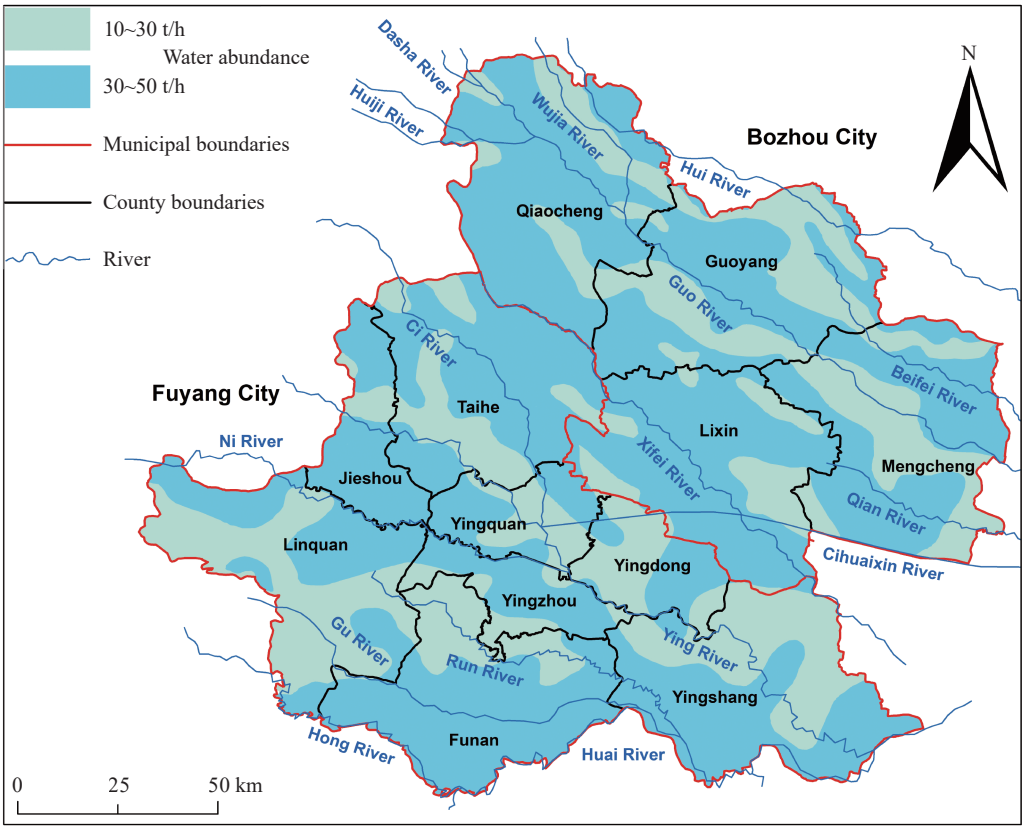


Fig. 1 The Western Part of the Huaibei Plain

the groundwater are primarily grayish-yellow, brown-yellow, and bluish-gray fine sands, very fine sands, and medium fine sands, all with a relatively loose structure. The deep aquifer group is composed of the upper part of the Neogene, buried at depths between 150 m and 350 m, and the groundwater is confined. The single layer thickness of the aquifer sands is substantial, and the lithology is mainly bluish-gray, grayish-white, and yellowish-gray medium sands, fine sands, and silt with a loose structure that is partially consolidated or semi-consolidated in some areas. The main aquifer group studied in this research was the shallow aquifer group.

1.3 Data

The main data used in this study include groundwater depth, lithology, and aquifer permeability coefficient, all of which are derived from the Hydrological Bureau of Anhui Provincial Department of Water Resources (https://slt.ah.gov.cn/tsdw/swj/szyshjjcypj/index.html). The Hydrological Bureau of Anhui Provincial Department of Water Resources has a comprehensive monitoring system to ensure the reliability and consistency of monitoring data.

2 Methodology

2.1 Weight analysis method

2.1.1 Analytic Hierarchy Process (AHP) method

The AHP method, proposed by Saaty (1983; 1987b), is a weight decision analysis method that breaks down the various elements involved in the decision-making process into different levels, such as objectives, criteria, and alternative options. Based on this, combined with qualitative and quantitative analysis methods, a comprehensive assessment of the elements at each level was conducted. The AHP method has a mature calculation approach and is widely applied. The key to determining the weights of each factor is to construct a judgment matrix, and it is recommended to refer to the publication of (Saaty, 1987a) for this process. This paper will not elaborate on the calculation principles.

2.1.2 Criteria importance through intercriteria correlation (CRITIC) method

The CRITIC method was proposed by Diakoulaki et al. (1995). The CRITIC method primarily measures the importance of different criteria based on their contrasting strengths and the degree of conflict between the criteria. In the context of the CRITIC method, the less conflict there is between criteria, the lower the weight is; simultaneously, the greater the positive correlation between two criteria, the less conflict there is, indicating that the two criteria reflect similar information in evaluating the merits. During the calculation process, the contrasting strength is multiplied by the conflict indicator and normalized to compute the weight of each criterion.

The CRITIC method calculates the weights of the criteria as follows:

$$\sigma_j = \sqrt{\frac{1}{n-1}\sum_{j=1}^{n}(x_j-\overline{x})^2} \tag{1}$$

$$r_{ij} = \frac{\sum_{i=1}^{n}\sum_{j=1}^{m}(x_i-\overline{x_i})(x_j-\overline{x_j})}{\sum_{i=1}^{n}\sum_{i=1}^{m}(x_i-\overline{x_i})^2(x_j-\overline{x_j})^2} \tag{2}$$

$$W_j = \sigma_j\sum_{i=1}^{n}(1-r_{ij}) \tag{3}$$

$$W_{CRIi} = \frac{W_i}{\sum_{i=1}^{k}W_i} \tag{4}$$

Where: x_i and x_j represent the values of indicators i and j, respectively; $\bar{x}_i$ and $\bar{x}_j$ represent the means of x_i and x_j, respectively; m and n are the number of sample data for indicators i and j; σ_j is the standard deviation; r_{ij} is the correlation coefficient; W_j is the information amount of indicator j; k is the number of indicators; and W_{CRIi} is the weight of indicator i.

2.1.3 Coefficient of variation method

The coefficient of variation, proposed by Karl Pearson, is a statistical tool for measuring the relative dispersion of data to evaluate the variability of different datasets. The principle of the coefficient of variation method is to determine the weight based on the amount of information reflected by the degree of variation in each evaluation criterion. This method links the weight of an indicator to its variability value, thereby fully reflecting the characteristics of the objective environment. It is a dynamic, objective weighting method that adjusts to changes in the environment. The approach to determine weights using the coefficient of variation method involves calculating the weights of different indicators within the system based on the

information they contain, followed by aggregating these weighted indicators for further calculation.

The formulas for calculating weights using the coefficient of variation method are as follows, as shown in Equations (5) and (6):

$$V_j = \frac{\sigma_j}{\bar{x}} \tag{5}$$

$$W_{CVj} = \frac{V_j}{\sum_{j=1}^{k} V_j} \tag{6}$$

Where: V_j represents the coefficient of variation for indicator j, and W_{CVj} represents the weight value calculated by the coefficient of variation method for indicator j.

2.1.4 Coupled weight method

To reduce the impact of any single weight calculation method on the evaluation results, this study employed a coupled approach using all three methods to determine the weights of the criteria, with the following expression, Equation (7):

$$W = \alpha W_{AHP} + \beta W_{CV} + \gamma W_{CRI} \tag{7}$$

Where: α, β, γ represents the weight of W_{AHP}, W_{CV}, W_{CRI}, respectively.

2.2 Sensitivity analysis

After determining the weights of evaluation indicators using a coupled method that integrates AHP, CRITIC, and the coefficient of variation method, it is necessary to verify the robustness of the weight configuration on the output results. To achieve this, the present study introduces Sensitivity Analysis (SA), which systematically perturbs the weights of each indicator to evaluate the response intensity of key indicators (e.g., distance to rivers) and identify highly sensitive weight parameters that significantly influence system behavior. This process ensures the robustness of the initial weight scheme. SA methods can be categorized based on their scope, applicability, and characteristics. The simplest and most common classification divides SA into local SA and global SA (Song et al., 2015). Local SA focuses on the impact of uncertain inputs around a single point (or baseline scenario), whereas global SA emphasizes the influence of uncertain inputs across the entire input space (Heng and Chen, 2013). Considering the interactions among evaluation indicators, this study adopts Global Sensitivity Analysis (GSA) to capture parameter interactions. After comparing the applicability and flexibility of various GSA methods (e.g., the Sobol method (Houle et al., 2017), EFAST method (Sahaar and Niemann, 2020), and Morris method (Wu et al., 2022)), a modified Morris method was selected to meet the practical needs of the research.

The classical Morris method designs an experimental matrix (e.g., Matrix B), altering one parameter value at a time to assess its independent impact, and calculates joint sensitivity by comparing output differences between specific rows. In the analysis of groundwater artificial recharge suitability conducted in this study, the Morris method was modified to efficiently identify key indicators and simplify calculations. Specifically, given five evaluation indicators, the method was adapted into a dual-factor sensitivity analysis framework. One "primary-varying indicator" (with a fixed direction of change) and one "secondary-varying indicator" (whose weight is perturbed) are selected simultaneously, while the weights of the remaining indicators remain unchanged. Adjustment rules ensure that the total weight of all indicators remains constant at 1 (as shown in Matrix B_1, where "1" represents a change). This modified approach preserves the core principles of the Morris method while significantly reducing computational complexity, making it more practical for real-world applications. It effectively reveals the impact trends of each indicator on recharge suitability, providing valuable support for subsequent research and engineering decision-making.

$$B = \begin{bmatrix} 0 & 0 & 0 & \cdots & 0 \\ 1 & 0 & 0 & \cdots & 0 \\ 1 & 1 & 0 & \cdots & 0 \\ \vdots & \vdots & \vdots & \ddots & \vdots \\ 1 & 1 & 1 & \cdots & 1 \end{bmatrix} \quad B1 = \begin{bmatrix} 0 & 0 & 0 & \cdots & 0 \\ 1 & 1 & 0 & \cdots & 0 \\ 1 & 0 & 1 & \cdots & 0 \\ \vdots & \vdots & \vdots & \ddots & \vdots \\ 1 & 0 & 0 & \cdots & 1 \end{bmatrix}$$

3 Results

The most critical part of this study is the establishment of an index system for the evaluation of the artificial groundwater recharge potential. By integrating the natural geographical, hydrometeorological, and regional hydrogeological conditions of the western part of the Huaibei Plain, five factors—the groundwater depth, the thickness of the drained aquifer, the permeability coefficient of the aquifer, the precipitation infiltration coefficient, and the distance to rivers—were selected as suitability evaluation indicators. The AHP, CRITIC, and coefficient of variation methods were each used to calculate the weights of the five indicators and determine their integrated weights. With the aid of the spatial analysis functions of the ArcGIS platform, the suitability for artificial

groundwater recharge in the study area was divided into several levels of potential.

3.1 Indices

(1) Groundwater depth (D). Groundwater depth refers to the vertical distance from the groundwater table to the ground surface, which is a key indicator for characterizing changes in groundwater storage. Previous studies (Hammouri et al., 2014; Sandoval and Tiburan, 2019) have confirmed that excessive exploitation of groundwater leads to a significant increase in depth, which can indirectly reflect the declining trend of regional groundwater levels. Based on the measured data of groundwater monitoring wells in the western Huaibei Plain in 2022, this study used the inverse distance weighting interpolation method to draw a spatial distribution map of groundwater depth. The locations of 196 monitoring wells are marked in Fig. 2a.

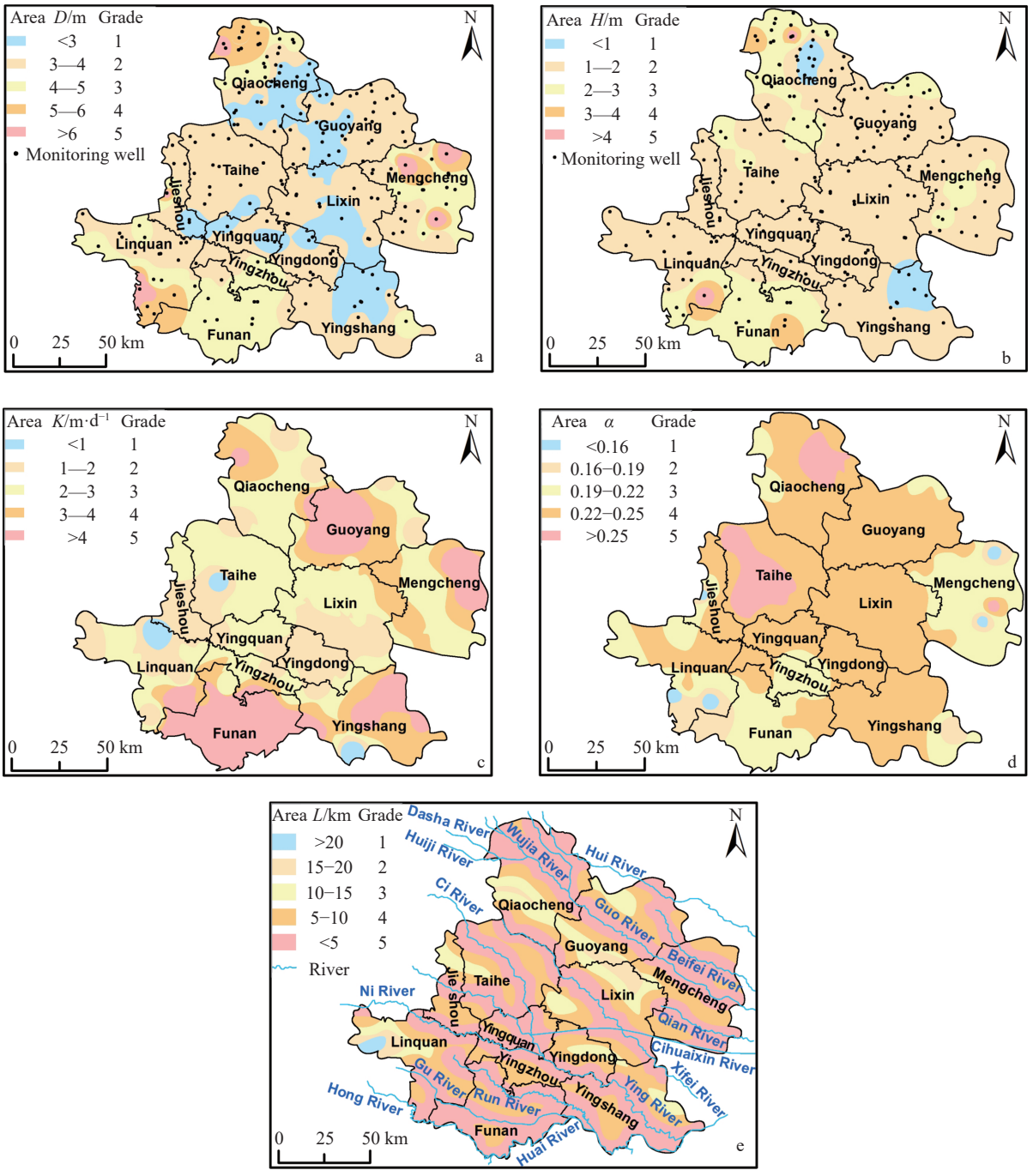


Fig. 2 Indicator grading scale (a: Groundwater depth, b: Thickness of drained aquifer, c: Permeability coefficient of aquifer, d: Precipitation infiltration coefficient, e: Distance to rivers)

The density of monitoring points is approximately 1.1 wells per 100 km^2. Although the spatial distribution shows a pattern of more points in the north and fewer in the south, the overall distribution is relatively uniform. The main soil type in the study area is Shajiang black soil, which has a high clay content, is rich in expansive clay minerals, has weak water permeability and air permeability, and is prone to drought, waterlogging and salinisation (Zhang et al., 2001). The dominant crops in the region are wheat and corn, and their suitable groundwater depth range for growth is 1–2 meters (Xu et al., 2024). Currently, the groundwater depth in the study area is generally 1.2–2.5 meters, which basically meets the growth needs of crops; however, the groundwater level will rise rapidly to within 1 meter during the flood season, posing an obvious risk of waterlogging (Lian et al., 2023; Wang and Ye, 2008). Considering key factors such as the capillary rise effect, water purification demand, and water resource carrying capacity during groundwater recharge, combined with regional hydrogeological conditions and ecological constraints of crop growth, this study divides groundwater depth into five suitability levels (Table 1).

(2) Thickness of drained aquifer (H). The thickness of the drained aquifer refers to the area where the groundwater level has dropped due to artificial extraction within the aquifer. Many researchers, such as Jena et al. (2020), generally use aquifer thickness or the thickness of the drained aquifer as evaluation indicators. This study argues that the thickness of the drained aquifer directly quantifies the available storage space for artificial recharge (the larger H is, the stronger the water storage capacity), and is associated with geological issues such as ground subsidence caused by overexploitation. Compared to traditional static aquifer thickness indicators (which only reflect natural water storage), it better fits the practical needs of the dynamic drained space in the western Huaibei Plain after long-term groundwater extraction; thus, the thickness of the drained aquifer can be regarded as a direct indicator of groundwater recharge suitability. In the western part of the Huaibei Plain, the groundwater extraction was minimal in 1980, which serves as the baseline for defining the initial state of the groundwater depth. By spatially superimposing and subtracting the groundwater depth distribution map of 1980 from the 2022 groundwater depth distribution map (Fig. 2a), a map depicting the thickness of the drained aquifer in the western part of the Huaibei Plain was generated (Fig. 2b). Based on a combination of the aquifer thickness and its spatial distribution, five grading intervals were established (Table 1).

(3) Permeability coefficient of aquifer (K). The permeability coefficient of the aquifer, also known as the hydraulic conductivity, describes the permeability of the aquifer medium. (Fan et al., 2023) argue that the permeability coefficient is a critical indicator for selecting suitable areas for artificial groundwater recharge. A higher permeability coefficient indicates that water moves more quickly through the stratum, thereby increasing the amount of water entering the aquifer and decreasing the likelihood of clogging. Additionally, a larger permeability coefficient suggests that the aquifer has a higher water-conducting capacity, which helps to improve the efficiency of artificial groundwater recharge. The permeability coefficients calculated from pumping tests (1980–2022) in the study area were used to generate a spatial distribution map of K using the inverse distance weighting method in the GIS platform (Fig. 2c). Based on the permeability coefficient valeus, they were divided into five grading intervals (Table 1).

(4) Precipitation infiltration coefficient (α). The precipitation infiltration coefficient reflects the efficiency of natural precipitation recharge to a certain extent. Rachdi et al. (2024) argue that lithological composition is crucial, as the vadose zone acts as a permeable and shallow buffer zone, facilitating rapid and substantial water recharge. This study, by superimposing vadose zone lithology with groundwater depth of the year 2022, combines "medium properties" and "hydrological

Table 1 Indicator scoring and grading table

Suitability Level	*D*		*H*		*K*		*α*		*L*	
	Grade/m	Score	Grade/m	Score	Grade/m·d^{-1}	Score	Grade	Score	Grade/km	Score
Optimal suitability	>6	5	>4	5	>4	5	>0.25	5	<5	5
High suitability	5–6	4	3–4	4	3–4	4	0.22–0.25	4	5–10	4
Moderate suitability	4–5	3	2–3	3	2–3	3	0.19–0.22	3	10–15	3
Low suitability	3–4	2	1–2	2	1–2	2	0.16–0.19	2	15–20	2
No suitability	<3	1	<1	1	<1	1	<0.16	1	>20	1

dynamics" to transcend the limitation of single lithological analysis (which only reflects "theoretical permeability"). It enables more accurate assessment of infiltration efficiency, contamination risk, engineering adaptability, and regional dynamic characteristics, providing a more comprehensive and reliable basis for the scientific selection of suitable areas for artificial groundwater recharge. By integrating the groundwater depth and the vadose zone lithology of the study area in the GIS platform, a distribution map of the precipitation infiltration coefficient for the study area was obtained (Fig. 2d). This map was then divided into five grading intervals (Table 1).

(5) Distance to rivers (*L*). Areas closer to rivers have higher importance and should be assigned higher spatial weights (Raja Shekar and Mathew, 2023). In this study, well-developed surface water bodies in the study area were used as water sources for artificial groundwater recharge, with a focus on the main stream of the Huaihe River, its first-level tributaries (such as the Guo River and Yinghe River), and second-level tributaries. Among them, the Yinghe River is the largest river in the study area, with a total length of 208 km within the territory and a controlled drainage area of 4,010 km^2. Euclidean distance analysis of rivers was conducted using the GIS platform, generating a distance distribution map from rivers in the study area (Fig. 2e). The effect of artificial groundwater recharge is significantly negatively correlated with the distance between the water source and the recharge area; the closer the distance, the higher the recharge efficiency. Conversely, not only will the project construction and operation costs be significantly increased, but also the risk of water source pollution during water conveyance will be increased, thereby threatening the water quality safety of the target aquifer (Gao, 2013). The study area features a well-developed fluvial system, dominated by the main stem of the Huai River and its first-order tributaries—the Guo River and Yinghe River—along with numerous second-order tributaries. All rivers in the region are characterized as lowland systems. Fluvial terraces are predominantly composed of alluvial low terraces, with widths ranging from 500 m to 1,000 m. In certain localized reaches, the boundaries between these terraces and the adjacent floodplains are indistinct. Moreover, during flood events, the terraces are frequently inundated. Considering terrace morphology and spatial continuity, the hydrological stability of potential groundwater recharge infrastructure, project investment feasibility, and the spatial distribution density of river networks across the study area, a 5 km buffer distance is determined to be the optimal and technically appropriate threshold for delineating recharge zones. Based on this, this study comprehensively considered technical, economic, and water quality safety factors, and divided the sutdy area into 5 equal-distance zones according to the distance from the water source (Table 1).

3.2 Indices weights

The judgment matrix derived from the expert scoring method for the five indicators was a 5 × 5 matrix (Table 2). The maximum eigenvalue λ_{max} = 5.0676 was calculated through consistency calculations, with a consistency index *CI* = 0.017 and an average random consistency index *CR* = 0.0151 < 0.1 (consistency test value, as referenced in the work of Maqbool et al. (2024)), which satisfies the consistency requirements. The calculated weights are shown in Table 2. The AHP method yielded the following order of the indicator weights: the thickness of the drained aquifer, the groundwater depth, the permeability coefficient of the aquifer, the precipitation infiltration coefficient, and the distance to rivers. The largest and smallest weight values were 0.417 and 0.062, respectively, with the largest weight being approximately 6.7 times the smallest.

Using the Band Set Statistics tool in the GIS platform, the correlation coefficients between various indicators were obtained, as shown in Table 3. The results indicate that there was a negative correlation between the depth of the groundwater and the precipitation infiltration coefficient, with a correlation coefficient of −0.60659. This suggests

Table 2 Judgment matrix and weights for evaluation indicators

Index	*H*	*D*	*K*	*α*	*L*	Weight
H	1	2	3	4	5	0.417
D	1/2	1	2	3	4	0.263
K	1/3	1/2	1	2	3	0.160
α	1/4	1/3	1/2	1	2	0.098
L	1/5	1/4	1/3	1/2	1	0.062

Table 3 Correlation coefficient and weight statistics table for evaluation indicators

Index	*D*	*H*	*K*	*α*	*L*	Weight
D	1.00000	0.50017	0.20964	−0.60659	0.12731	0.227
H	0.50017	1.00000	0.26631	−0.37925	0.10943	0.152
K	0.20964	0.26631	1.00000	−0.26355	0.05371	0.196
α	−0.60659	−0.37925	−0.26355	1.00000	−0.06245	0.269
L	0.12731	0.10943	0.05371	−0.06245	1.00000	0.156

that in the same area, the greater the depth of the groundwater, the smaller the precipitation infiltration coefficient, making it difficult to have both. However, the depth of the groundwater was positively correlated with indicators such as the thickness of the drained aquifer. For instance, the correlation coefficient with the thickness of the drained aquifer was 0.50017, indicating that in the same area, the greater the depth of the groundwater, the greater the thickness of the drained aquifer. Based on the CRITIC method (formulas (1) – (4)), the weights of each evaluation indicator were calculated, as shown in Table 3. The CRITIC method yielded the following order of indicator weights in terms of importance: the precipitation infiltration coefficient, the groundwater depth, the permeability coefficient of the aquifer, the distance to rivers, and the thickness of the drained aquifer. The precipitation infiltration coefficient had the largest weight at 0.269, while the thickness of the drained aquifer had the smallest weight at 0.152.

The weights of each indicator calculated using the coefficient of variation method are presented in Table 4. The coefficient of variation method yielded the following order of the indicator weights in terms of magnitude: The distance to rivers (0.282), the thickness of the drained aquifer (0.192), the precipitation infiltration coefficient (0.188), groundwater depth (0.176), and the permeability coefficient of the aquifer (0.162). The largest and smallest weights were 0.282 and 0.162, respectively, with relatively small differences in the weight values between the indicators.

Table 4 Coefficient of variation method weight statistics table

Index	*D*	*H*	*K*	*α*	*L*
Weight	0.176	0.192	0.162	0.188	0.282

A comprehensive comparison of the weights calculated by the Analytic Hierarchy Process (AHP), CRITIC method, and coefficient of variation method shows that under the premise of an average value of 0.2, their standard deviations are 0.128, 0.044, and 0.042, respectively. This indicates that the weights derived from objective weighting methods based on data have smaller fluctuations, while subjective weighting methods are greatly influenced by factors such as the researchers, leading to significant differences in the weights of various indicators. The coupling of weights can help eliminate such discrepancies. In Equation (7), α, β, and γ represent the coefficients used in the weight calculation method, with the sum of these coefficients equaling 1. Following the equal distribution principle, the coefficients were assigned equal values, specifically $\alpha = \beta = \gamma = 1/3$. The weights of the evaluation indicators, calculated using the combined weight calculation method, are presented in Table 5.

Table 5 Coupled weight table for evaluation indicators

Index	*D*	*H*	*K*	*α*	*L*
W_{AHP}	0.263	0.417	0.160	0.098	0.062
W_{CRI}	0.227	0.152	0.196	0.269	0.156
W_{CV}	0.176	0.192	0.162	0.188	0.282
W	0.222	0.254	0.173	0.185	0.166

The weight for the distance to rivers calculated using the AHP was 0.062, the smallest among the five indicators. The distance to rivers directly affects the water conveyance costs for artificial groundwater recharge and is a key factor in assessing the economic feasibility; thus, its relatively low weight is noteworthy. The CRITIC method determined the highest weight for the precipitation infiltration coefficient at 0.269, while the thickness of the drained aquifer received the lowest weight. The thickness of the drained aquifer measures the size of the water storage space; without it the difficulty in replenishing groundwater must be directly determined. Therefore, the weight assigned by the CRITIC method to the thickness of the drained aquifer is considered to be on the low side. The coefficient of variation method calculated the highest weight for the distance to rivers (0.282) and the lowest weight for the permeability coefficient of the aquifer (0.162). The goal of artificial groundwater recharge is to increase the storage of groundwater by infiltrating excess surface water into the ground. The distance to rivers affects the cost of

the project and should not be the primary factor affecting artificial groundwater recharge. Consequently, it was found that the weight calculation results from the AHP, CRITIC, and coefficient of variation methods were not entirely consistent. The combined weight calculation method ranked the indicator weights from largest to smallest as follows: the thickness of the drained aquifer, the depth of the groundwater, the precipitation infiltration coefficient, the permeability coefficient of the aquifer, and the distance to rivers. The thickness of the drained aquifer and the groundwater depth directly determine whether there is storage space for artificial groundwater recharge and how much the groundwater can be increased. The combined weight calculation method assigned weights of 0.254 and 0.222 to these two indicators, respectively, which are more reasonable in terms of the weight order and magnitude compared to the individual calculation method results.

3.3 Classification of artificial groundwater recharge suitability and potential levels

When only the depth of the groundwater or the thickness of the drained aquifer (Fig. 2a and Fig. 2b) were considered, nearly 40% of the study area had a moderate level of suitability for artificial groundwater recharge, with fewer areas of high and very high suitability. When analyzing the permeability coefficient of the aquifer alone, the overall potential for artificial recharge in the study area was quite good, with moderate, high, and very high suitability potential areas accounting for about 80% of the study area. Analyzing the precipitation infiltration coefficient revealed that there were areas of high recharge suitability in places like Taihe, Guoyang, Lixin, and YingShang, with fewer areas of moderate suitability. Water source conditions mainly rely on well-developed river systems within the study area, with high and very high recharge suitability areas distributed along corresponding rivers such as the Huai River and Gu River. Based on a single indicator, the distribution of the suitability potential for artificial groundwater recharge varied across the study area.

The suitability and potential for artificial groundwater recharge depend on multiple factors. Based on the coupled weight calculation method for the weights of each indicator, and with the aid of the spatial analysis functions of the ArcGIS platform, the suitability and potential levels for artificial groundwater recharge were determined. Spatial analysis operates on the principle of weighting. It involves two main steps. First, each evaluation indicator's raster data is multiplied by the indicator's corresponding weight. Second, the weighted raster data from all indicators are summed to generate the output raster. This yields a score indicating the suitability and potential of artificial groundwater recharge in the western Huaibei Plain. For ease of understanding, this study defines the scoring value as β. With reference to the research findings of Wang et al. (2024), this study uses the natural breaks method to classify the comprehensive score values. This is an objective classification technique based on the inherent distribution characteristics of the data. Its core logic involves identifying "natural breakpoints" in the data through mathematical optimization, such that differences within each class are minimized (small within-class variance) and differences between classes are maximized (large between-class variance). Specifically, this method minimizes the Within-Class Sum of Squares (WCSS) and maximizes the Between-Class Sum of Squares (BCSS) through iterative calculations, thereby highlighting the natural grouping patterns of the data. Based on the actual distribution pattern of the comprehensive score β, the method automatically identifies "cluster boundaries" in the dataset. Using the natural breaks classification, the recharge suitability is divided into four levels (Fig. 3), namely high recharge potential (β>3.55), moderate recharge potential (3.14<β<3.55), low recharge potential (2.79<β<3.14 points), and no recharge potential (β<2.79).

Fig. 3 and Fig. 4 indicate that the areas with high and moderate suitability potential for groundwater recharge in the western part of the Huaibei Plain were primarily located in the southern part of Fuyang County, the northern part of Qiaocheng District, the central part of Guoyang County, and the northeastern part of Mengcheng County, with some distribution in Taihe and Yingshang. These areas accounted for 32.93% of the study area. The groundwater depth and the thickness of the drained aquifer in these regions are relatively large, providing good water storage space, and the aquifer permeability coefficient is also high, indicating a strong water conduction capacity. Areas with low suitability potential for groundwater recharge were found surrounding the moderately suitable areas, as well as in Lixin County and Yingquan District, covering 41.25% of the study area. The remaining areas were considered unsuitable for recharge, making up 25.82% of the study area, mainly due to the low thickness of the drained aquifer. Based on five evaluation indicators—the groundwater depth,

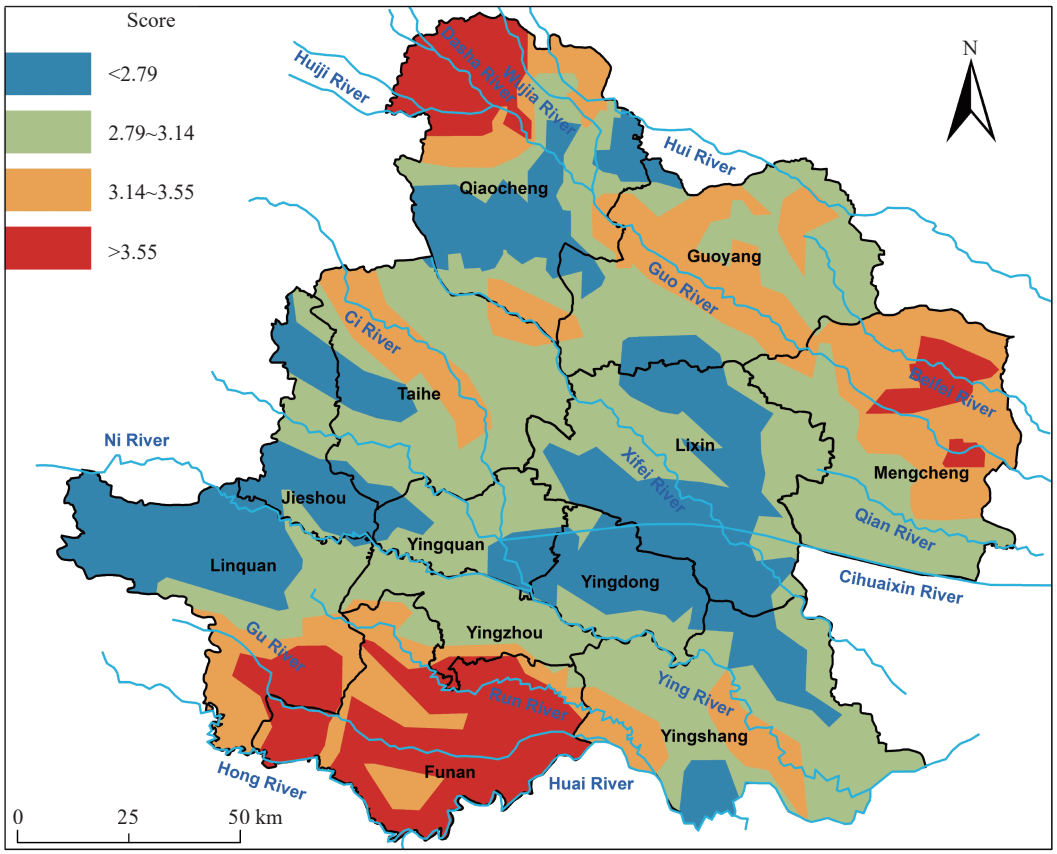


Fig. 3 Comprehensive suitability potential score

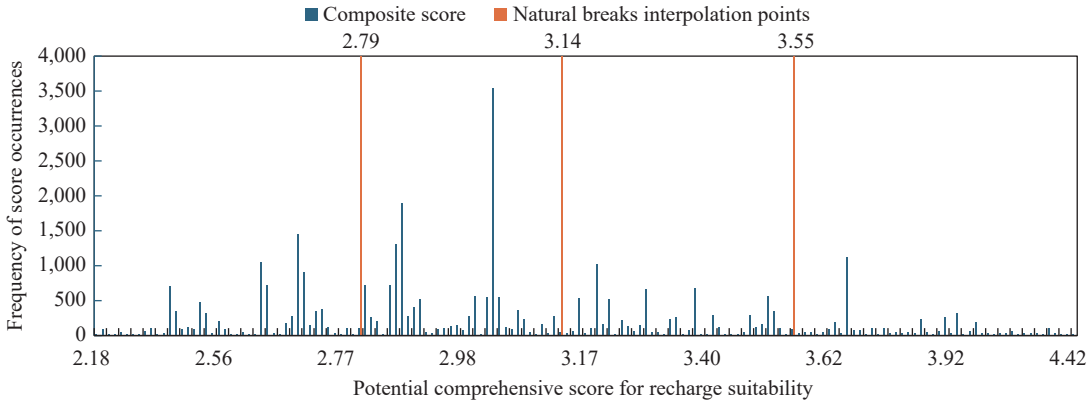


Fig. 4 Comprehensive suitability potential score distribution

the thickness of the drained aquifer, the aquifer permeability coefficient, the precipitation infiltration coefficient, and the water source distance—the zoning results for the suitability of artificial groundwater recharge were relatively reasonable.

3.4 Sensitivity analysis of groundwater indicator weights

To further evaluate the influence of indicator weights on the classification of groundwater artificial recharge potential, this study performed a sensitivity analysis of the indicator weights using a simplified Morris method. The analysis focused on five indicators: groundwater burial depth (D), thickness of the dewatered aquifer (H), aquifer permeability coefficient (K), precipitation infiltration coefficient (α), and distance from rivers (L). Given that the sum of the weights of these five indicators equals 1, analyzing the impact of a single parameter's change on the evaluation results is not feasible. Consequently, based on the principle of permutation and combination, 40 sets of indicator weights were generated through pairwise combinations.

During the calculation process, taking groundwater burial depth (D) and thickness of the dewatered aquifer (H) as examples, the original weights of D and H were denoted as W_{D0} and W_{H0}, respectively. After adjustment, the weights became W_{D1} and W_{H1}. For instance, if the weight of indicator D increased by 20%, then:

$$W_{D1} = W_{D0} + 20\% \times W_{D0}$$
$$W_{H1} = W_{H0} - 20\% \times W_{D0} \quad (8)$$

Similarly, the weights of other pairwise-adjusted indicators were derived, as shown in the following matrix (in matrix $B_i^{\pm}$, i represents the indicator with the primary weight change, namely D, H, K, α, and L; ± indicates that the weight of the primary changing indicator is increased or decreased by 20%). For each combination of adjusted weights, the groundwater artificial recharge suitability potential scores for the study area were calculated using the spatial analysis capabilities of the ArcGIS platform. The proportions of the study area classified as no potential, low potential, medium potential, and high potential zones for groundwater artificial recharge were statistically analyzed (Fig. 5).

$$BD^{+} = \begin{bmatrix} 0.222 & 0.254 & 0.173 & 0.185 & 0.166 \\ 0.266 & 0.210 & 0.173 & 0.185 & 0.166 \\ 0.266 & 0.254 & 0.129 & 0.185 & 0.166 \\ 0.266 & 0.254 & 0.173 & 0.141 & 0.166 \\ 0.266 & 0.254 & 0.173 & 0.185 & 0.122 \end{bmatrix}$$

$$BD^{-} = \begin{bmatrix} 0.222 & 0.254 & 0.173 & 0.185 & 0.166 \\ 0.178 & 0.298 & 0.173 & 0.185 & 0.166 \\ 0.178 & 0.254 & 0.217 & 0.185 & 0.166 \\ 0.178 & 0.254 & 0.173 & 0.229 & 0.166 \\ 0.178 & 0.254 & 0.173 & 0.185 & 0.210 \end{bmatrix}$$

$$BH^{+} = \begin{bmatrix} 0.222 & 0.254 & 0.173 & 0.185 & 0.166 \\ 0.171 & 0.305 & 0.173 & 0.185 & 0.166 \\ 0.222 & 0.305 & 0.122 & 0.185 & 0.166 \\ 0.222 & 0.305 & 0.173 & 0.134 & 0.166 \\ 0.222 & 0.305 & 0.173 & 0.185 & 0.115 \end{bmatrix}$$

$$BH^{-} = \begin{bmatrix} 0.222 & 0.254 & 0.173 & 0.185 & 0.166 \\ 0.273 & 0.203 & 0.173 & 0.185 & 0.166 \\ 0.222 & 0.203 & 0.224 & 0.185 & 0.166 \\ 0.222 & 0.203 & 0.173 & 0.236 & 0.166 \\ 0.222 & 0.203 & 0.173 & 0.185 & 0.217 \end{bmatrix}$$

$$BK^{+} = \begin{bmatrix} 0.222 & 0.254 & 0.173 & 0.185 & 0.166 \\ 0.187 & 0.254 & 0.208 & 0.185 & 0.166 \\ 0.222 & 0.219 & 0.208 & 0.185 & 0.166 \\ 0.222 & 0.254 & 0.208 & 0.150 & 0.166 \\ 0.222 & 0.254 & 0.208 & 0.185 & 0.131 \end{bmatrix}$$

$$BK^{-} = \begin{bmatrix} 0.222 & 0.254 & 0.173 & 0.185 & 0.166 \\ 0.257 & 0.254 & 0.138 & 0.185 & 0.166 \\ 0.222 & 0.289 & 0.138 & 0.185 & 0.166 \\ 0.222 & 0.254 & 0.138 & 0.220 & 0.166 \\ 0.222 & 0.254 & 0.138 & 0.185 & 0.201 \end{bmatrix}$$

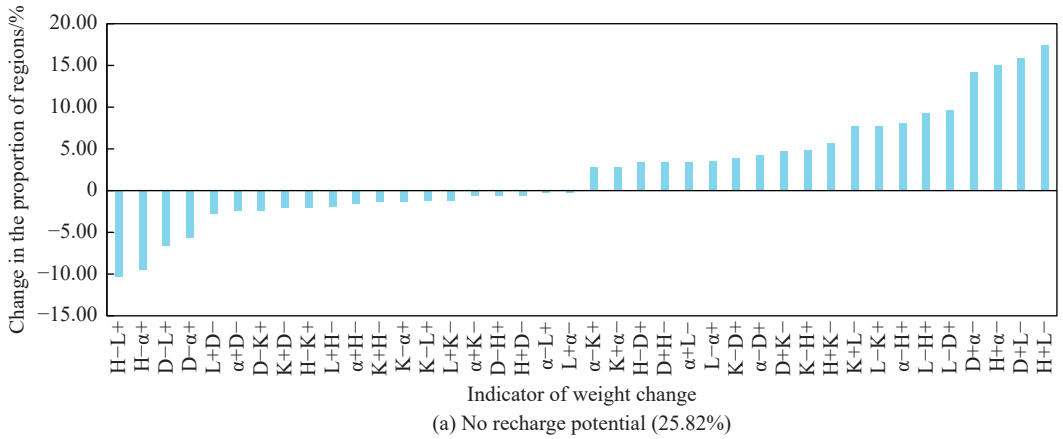
$$B\alpha^{+} = \begin{bmatrix} 0.222 & 0.254 & 0.173 & 0.185 & 0.166 \\ 0.185 & 0.254 & 0.173 & 0.222 & 0.166 \\ 0.222 & 0.217 & 0.173 & 0.222 & 0.166 \\ 0.222 & 0.254 & 0.136 & 0.222 & 0.166 \\ 0.222 & 0.254 & 0.173 & 0.222 & 0.129 \end{bmatrix}$$

$$B\alpha^{-} = \begin{bmatrix} 0.222 & 0.254 & 0.173 & 0.185 & 0.166 \\ 0.259 & 0.254 & 0.173 & 0.148 & 0.166 \\ 0.222 & 0.291 & 0.173 & 0.148 & 0.166 \\ 0.222 & 0.254 & 0.210 & 0.148 & 0.166 \\ 0.222 & 0.254 & 0.173 & 0.148 & 0.203 \end{bmatrix}$$

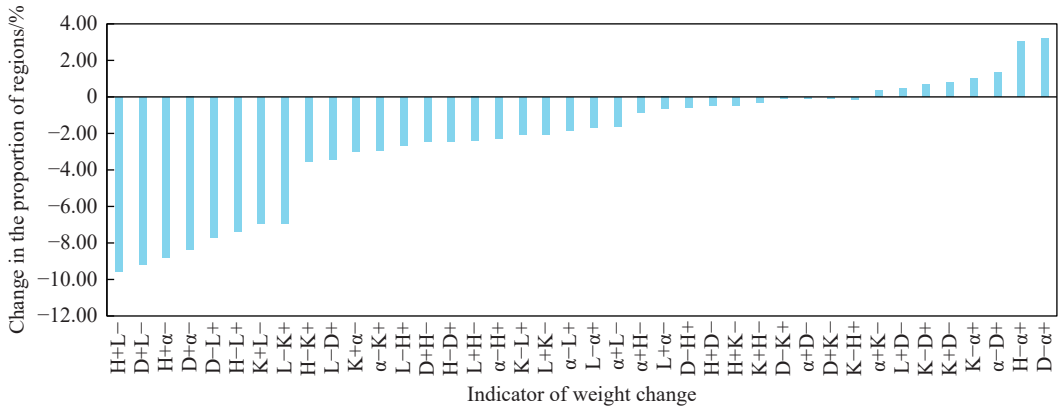
$$BL^{+} = \begin{bmatrix} 0.222 & 0.254 & 0.173 & 0.185 & 0.166 \\ 0.189 & 0.254 & 0.173 & 0.185 & 0.199 \\ 0.222 & 0.221 & 0.173 & 0.185 & 0.199 \\ 0.222 & 0.254 & 0.140 & 0.150 & 0.199 \\ 0.222 & 0.254 & 0.173 & 0.185 & 0.199 \end{bmatrix}$$

$$BL^{-} = \begin{bmatrix} 0.222 & 0.254 & 0.173 & 0.185 & 0.166 \\ 0.255 & 0.254 & 0.173 & 0.185 & 0.133 \\ 0.222 & 0.287 & 0.173 & 0.185 & 0.133 \\ 0.222 & 0.254 & 0.206 & 0.185 & 0.133 \\ 0.222 & 0.254 & 0.173 & 0.218 & 0.133 \end{bmatrix}$$

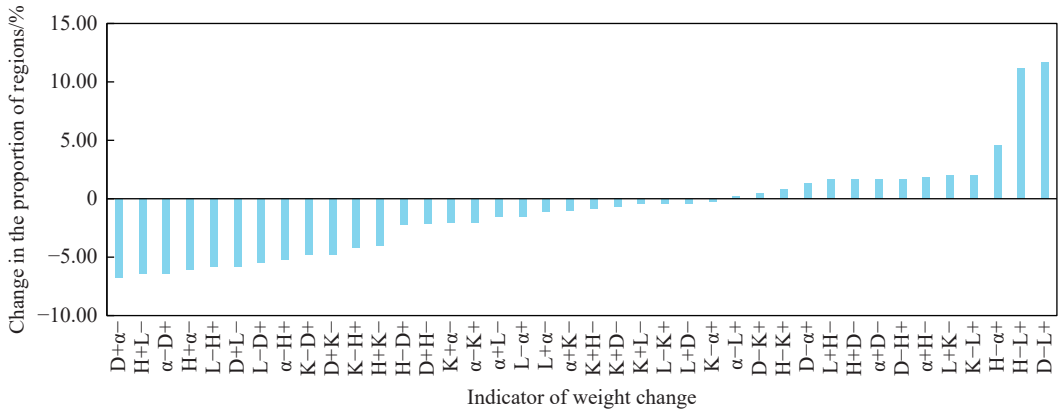
A preliminary analysis of Fig. 5 (Taking Fig. 5(a) as an example, the column labeled D+H− represents a 3.44% increase in the proportion of non-potential zones after weight adjustment, while the column labeled D-H+ represents a 0.58% decrease in the proportion of non-potential zones after weight adjustment) reveals that when the weight of H decreased and the weight of L increased, the proportion of high-potential zones surged to 17.80%, representing an increase of 57.92% compared to the initial state, while the proportion of no-potential zones decreased from 25.82% to 15.50%. This indicates that the proximity to river water sources and relaxed storage constraints synergistically enhance recharge potential. Conversely, when the weight of H increased and the weight of L decreased, the proportion of no-potential zones soared to 43.26%, while high-potential zones sharply decreased by 1.40%, representing a 12.42% reduction compared to the initial state This highlights that the negative interaction between water source availability and storage constraints severely inhibits suitability. When the weight of K increased and the weight of H decreased, the proportion of high-potential zones increased by 22.63% compared to the initial state, while no-potential zones remained stable at 24.49%. This suggests that enhancing hydraulic conductivity while relaxing storage constraints optimizes recharge efficiency. When the weight of H increased and the weight of K decreased, the proportion of no-potential zones rose to 31.47%, and medium-potential zones were compressed to 17.65%. This reflects the combined limitations of



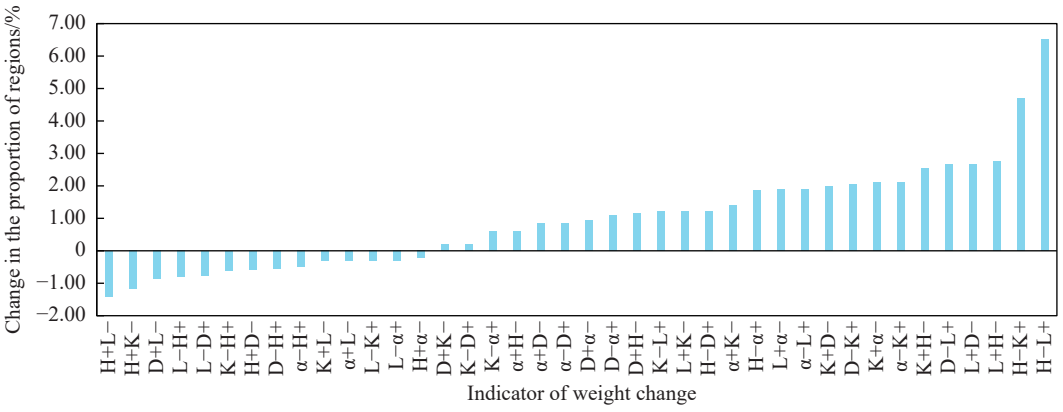
(a) No recharge potential (25.82%)



(b) Low recharge potential (41.25%)



(c) Moderate recharge potential (21.66%)



(d) High recharge potential (11.27%)

Fig. 5 Variation in proportion of suitability potential zones

inadequate hydraulic conductivity and stringent storage constraints.

Adjustments to groundwater burial depth (*D*) and infiltration coefficient (*α*) as primary-varying indicators had a weaker impact on potential zones; however, their combinations affected the identification of no-potential zones to some extent. The combination of *H* and *L* significantly influenced changes in all potential zones. Pairing *K* with any indicator resulted in relatively stable fluctuations in the distribution of potential zones. Therefore, in practical applications, priority should be given to optimizing the weights of *L* and *K*, while dynamically adjusting *H* to adapt to regional conditions.

Based on the change rates of high-potential zones (Table 6), the sensitivity of the five indicators ranked from highest to lowest as follows: Distance from rivers (*L*) > aquifer permeability coefficient (*K*) > thickness of the dewatered aquifer (*H*) > precipitation infiltration coefficient (*α*) > groundwater burial depth (*D*). This sensitivity ranking implies that increasing the weight of *L* while decreasing the weight of *H* emphasizes the availability of recharge water sources. Without a reliable water source, even if other parameters meet the recharge conditions, recharge remains unfeasible. Thus, changes in the weight of *L* drive a surge in high-potential zones. Increasing the weight of *K* while decreasing the weight of *H* highlights the synergy between hydraulic conductivity efficiency and storage space optimization during recharge. If hydraulic conductivity is insufficient, even ample storage space cannot ensure efficient recharge. Therefore, this combination significantly expands high-potential zones. Increasing the weight of *K* while decreasing the weight of α underscores the dominance of aquifer hydraulic conductivity over surface infiltration conditions. If water transport efficiency is inadequate, strong surface infiltration capacity alone cannot guarantee sustainable recharge. Thus, prioritizing *K* directly enhances suitability. Decreasing the weight of *H* while increasing the weight of *D* emphasizes the precise alignment of storage conditions with burial depth constraints. If burial depth does not meet moderate requirements (too shallow or too deep), the advantages of storage space cannot be effectively utilized. Hence, this combination enhances the quality of potential zones through refined screening.

The sensitivity analysis results from the 40 groups of indicator weights revealed the following common patterns in the response of evaluation results to weight changes:

(1) High-potential zones are the core response target: The area proportion of high-potential zones exhibited the largest change rate (−12.42% to 57.92%), directly reflecting the sensitivity of evaluation results to weight adjustments.

(2) Low-potential zones are the most stable: The area proportion of low-potential zones fluctuated within the smallest range (31.67% to 44.46%), indicating strong resistance to interference in identifying basic suitability areas.

(3) No-potential zones fluctuate substantially: The proportion ranged from 15.50% to 43.26%, primarily influenced by the synergistic adjustments of indicators *L*, *H*, and *D*.

(4) Medium and high-potential zones show coordinated expansion/contraction trends: The proportions of medium and high-potential zones often changed synchronously (e.g., when *L*+ and *H*−, medium-potential zones increased from 21.66% to 23.29%, and high-potential zones increased from 11.27% to 14.04%). This reflects the continuity of recharge conditions between these zones.

In summary, the model for evaluating groundwater artificial recharge potential zones in the study area demonstrated good overall stability.

Table 6 Change rates of high-potential zones

	D+H−	***D-H+***	***D+K−***	***D-K+***	***D+α−***	***D-α+***	***D+L−***	***D-L+***
Rate	10.24%	−4.95%	1.67%	18.27%	8.23%	9.77%	−7.74%	23.78%
	H+D−	*H-D+*	*H+K−*	*H-K+*	*H+α−*	*H-α+*	*H+L−*	*H-L+*
Rate	−5.08%	10.84%	−10.44%	41.69%	−1.92%	16.46%	−12.42%	57.92%
	K+D−	*K-D+*	*K+H−*	*K-H+*	*K+α−*	*K-α+*	*K+L−*	*K-L+*
Rate	17.56%	1.82%	22.63%	−5.31%	18.79%	5.27%	−2.88%	10.79%
	α+D−	*α-D+*	*α+H−*	*α-H+*	*α+K−*	*α-K+*	*α+L−*	*α-L+*
Rate	7.55%	7.63%	5.43%	−4.42%	12.31%	18.79%	−2.88%	16.83%
	L+D−	*L-D+*	*L+H−*	*L-H+*	*L+K−*	*L-K+*	*L+α−*	*L-α+*
Rate	23.78%	−6.75%	24.62%	−7.17%	10.79%	−2.88%	16.78%	−2.88%

Despite fluctuations in the proportion of high-potential zones (initial: 11.27%, maximum: 17.80%), the proportions of low-potential (41.25% ± 5%) and medium-potential (21.66% ± 5%) zones remained relatively stable. The evaluation results did not undergo disruptive changes, verifying the model's tolerance to weight fluctuations. Additionally, sensitive combinations to avoid during weight adjustments include: Negative adjustments (decreasing one indicator's weight while increasing the associated indicator's weight), such as: $L-$ and $H+$ (high-potential zones decreased by 12.42%), $K-$ and $H+$ (high-potential zones decreased by 10.44%) and $L-$ and $\alpha+$ (high-potential zones decreased by 2.88%).

4 Discussion

(1) Evaluation methods and advantages

This study systematically evaluated the suitability of artificial groundwater recharge in the western part of the Huaibei Plain by constructing a subjective-objective coupled multi-criteria decision-making framework (coupling the Analytic Hierarchy Process (AHP), coefficient of variation method, and CRITIC method). The selection of evaluation indicators is reasonable, and the inverse distance weighting method used in the classification process has a relative error controlled within 10%, which verifies the reliability of the interpolation results and can meet the spatial analysis requirements for groundwater recharge suitability evaluation. The subjective-objective coupled method breaks through the limitations of traditional single-weight methods: It not only avoids potential empirical biases of subjective methods such as AHP but also mitigates the shortcomings of objective methods (e.g., CRITIC method's reliance on data quality and the coefficient of variation method's susceptibility to outliers), significantly improving the scientific rigor of indicator weight allocation (groundwater depth: 0.222; thickness of drained aquifer: 0.254; permeability coefficient of aquifer: 0.173; precipitation infiltration coefficient: 0.185; distance to rivers: 0.166). It provides a replicable methodological reference for evaluating recharge suitability under complex hydrogeological conditions. Meanwhile, the high-sensitivity indicators identified by sensitivity analysis provide directions for improvement for the subsequent adjustment and optimization of the groundwater recharge suitability evaluation model.

(2) Patterns of recharge potential zones

The study identified high- and medium-potential recharge areas accounting for 32.93% of the study area through GIS spatial analysis, primarily distributed along the Guo River and Shaying Rivers in regions such as southern Fuyang County and northern Qiaocheng District. Fig. 1 presents the groundwater-richness zoning map of the study area, revealing that the aquifers within the identified high- and medium-potential zones exhibit pronounced water-bearing capacity. Consistent with this, Fig. 2 indicates that the groundwater depth in these zones ranges from 5 m to 6 m, and the hydraulic conductivity is relatively high. These hydrogeological characteristics provide a robust physical basis for artificial groundwater recharge, thereby corroborating the rationality of the delineated high- and medium-potential recharge zones. Additionally, these high- and medium-potential areas show notable spatial consistency with current regional groundwater management practices: The recent comprehensive groundwater over-exploitation control project implemented in Fuyang City (e.g., sealing deep groundwater wells and drilling new shallow groundwater wells) has designated regions such as Linquan County and Yingshang County as key governance areas (https://www.fy.gov.cn/OpennessContent/show/2277354.html), which highly align with the "surface water replacement for deep groundwater" restoration goals of the high-potential areas; projects such as the high-quality water source replacement project in Mengcheng County, Bozhou City (https://slj.bozhou.gov.cn/News/show/632931.html), which covers the Guohe River Basin, overlap with the distribution of high-potential areas and can provide stable surface water sources for artificial recharge. Furthermore, the stability pattern of potential area proportions ("low-potential areas > medium-potential areas > high-potential areas") verified by sensitivity analysis further consolidates the reliability of the suitability zoning results.

(3) Existing challenges

However, the practical implementation of high- and medium-potential areas still faces multiple challenges. First, insufficient coordination of engineering facilities: Current comprehensive governance projects in Fuyang City focus on "sealing old wells and building new pipelines" (e.g., 19.97 km of water supply pipelines have been laid in Linquan County), but infiltration facilities required for artificial recharge (e.g., ecological ditches, artificial infiltration pits) have not been explicitly included in construction plans, potentially reducing the coordination efficiency between water transfer projects and recharge facilities. Second, prominent competition for surface water sources: Surface water sources in the western Huaibei Plain

currently prioritize domestic and agricultural irrigation needs (e.g., water from the South-to-North Water Diversion Project is prioritized for residential use), which may limit the water allocation scale for artificial recharge. Although rainfall infiltration is a natural recharge method, deep groundwater distribution areas (e.g., Funan County) rely on ditch and pond seepage recharge, and reduced surface runoff during dry seasons will further exacerbate recharge water shortages. Third, significant difficulty in multi-objective coordination: Implementing recharge projects in high-potential areas requires simultaneously meeting goals such as "artificial groundwater recharge," "surface water replacement," and "agricultural irrigation," creating substantial coordination pressures among social, environmental, and management needs.

(4) Strategies and prospects

To address these challenges, solutions can be gradually advanced. First, synchronize the planning of infiltration facilities with water supply pipeline construction (e.g., pilot "water supply pipeline-infiltration pit cluster" joint projects along the Guo River and Shaying Rivers) to enhance the coordination efficiency of "water transfer-recharge." Second, explore a "multi-source recharge" strategy by utilizing surplus surface water during wet seasons for concentrated recharge and testing safe recharge technologies using reclaimed water (e.g., tailwater from urban sewage treatment plants) to expand water sources. Third, introduce a "multi-objective optimization model" to dynamically adjust recharge plans based on regional water use patterns (e.g., prioritizing water allocation for recharge during non-irrigation periods in agriculture) and balance various needs.

Overall, this study not only provides scientific evidence for artificial groundwater recharge in the western Huaibei Plain but also offers a referential framework for water resource management in similar regions through its "empirical knowledge-data-driven" integrated evaluation approach. In the future, by adding long-term hydrogeological monitoring stations, incorporating remote sensing data to improve data accuracy, constructing a "natural-social" dual-dimensional evaluation model with socioeconomic data, and conducting cross-basin comparative studies to optimize method parameters, it is expected to further promote the development of groundwater recharge toward "precision and efficiency".

5 Conclusions

This study systematically assessed the suitability of surface infiltration–based artificial groundwater recharge in the western Huaibei Plain, China, utilizing a rigorously structured multi-criteria decision-making framework. Distinct from prior single-method assessments conducted in the region, this approach ensures both methodological transparency and result objectivity through an integrated weight-determination strategy—combining objective weighting with hydrogeological interpretability to mitigate subjectivity in indicator prioritization. Five physically meaningful and operationally tractable evaluation indicators were selected: Groundwater depth (0.222), thickness of the saturated aquifer system (0.254), aquifer permeability coefficient (0.173), precipitation infiltration coefficient (0.185), and distance to perennial rivers (0.166). All weights were derived via coupled method analysis—a statistically robust, data-driven method that eliminates reliance on expert judgment alone and enhances cross-study comparability.

Spatial evaluation results identified high- and medium-potential recharge zones covering 32.93% of the study area, with pronounced spatial clustering along the Guo River and Shaying River corridors—including southern Fuyang County and northern Qiaocheng District. These zones exhibit favorable hydrogeological attributes. Critically, their spatial alignment directly supports the primary management objective of mitigating chronic groundwater over-exploitation in the region. To evaluate result stability, a comprehensive sensitivity analysis was performed by perturbing each indicator's weight within ±20% of its baseline value; results demonstrated consistent rank-order preservation across potential classes (low > medium > high).

Drawing on these findings, three evidence-informed implementation recommendations are advanced: (1) Prioritize iterative calibration of weights for highly sensitive indicators—particularly K (permeability coefficient) and L (distance to rivers)—during model deployment to enhance spatial discrimination accuracy for high-yield recharge zones; (2) Adopt a zonal weight-adaptation protocol wherein indicator *L* is assigned elevated weight (e.g., +0.05–0.10) in riparian subzones, thereby improving model responsiveness to localized hydrological connectivity; and (3) Strategically concentrate pilot-scale recharge infrastructure development in high-suitability corridors—especially along the Guo and Shaying Rivers—to optimize hydraulic efficiency, accelerate aquifer recovery, and deliver measurable reductions in regional groundwater overdraft.

This study delivers a spatially explicit, statistically validated suitability zoning map for artificial groundwater recharge across the western Huaibei Plain. It provides both an empirical foundation and a replicable methodological framework for evidence-based recharge planning in alluvial plains. A key limitation lies in its static nature: While capturing baseline hydrogeological conditions, the current framework does not explicitly incorporate temporal dynamics—such as seasonal fluctuations in groundwater depth, antecedent moisture conditions, or interannual variability in precipitation infiltration. Future research should integrate time-series hydrological data with transient numerical modeling (e.g., MODFLOW coupled with recharge flux estimation) to develop dynamic suitability indices and predictive capacity assessments—thereby advancing from static suitability mapping toward adaptive, performance-integrated groundwater resource governance.

Acknowledgments

This work was supported by the Anhui Provincial Natural Science Foundation (No. 2408085MD093). Data used to produce this paper are available on contact of the first author.

References

Agarwal R, Garg PK. 2016. Remote sensing and GIS based groundwater potential & recharge zones mapping using multi-criteria decision making technique. Water Resources Management, 30: 243−260. DOI：10.1007/s11269-015-1159-8.

Ajjur SB, Mogheir YK. 2019. Identification of intrinsic suitable sites in Gaza Strip for the application of artificial groundwater recharge using a geographic information system multi-criteria decision analysis. Journal of Multi-Criteria Decision Analysis, 27: 255−265. DOI：10.1002/mcda.1701.

Aju CD, Achu AL, Raicy MC, et al. 2021. Identification of suitable sites and structures for artificial groundwater recharge for sustainable water resources management in Vamanapuram River Basin, South India. HydroResearch, 4: 24−37. DOI：10.1016/j.hydres.2021.04.001.

Aloui D, Chekirbane A, Stefan C, et al. 2022. Use of a GIS-multi-criteria decision analysis and web-based decision support tools for mapping and sharing managed aquifer recharge feasibility in Enfidha plain, NE of Tunisia. Arabian Journal of Geosciences, 15: 658. DOI：10.1007/s12517-022-09893-8.

Arya S, Subramani T, Karunanidhi D. 2020. Delineation of groundwater potential zones and recommendation of artificial recharge structures for augmentation of groundwater resources in Vattamalaikarai Basin, South India. Environmental Earth Science, 79: 102. DOI：10.1007/s12665-020-8832-9.

Biswas G, Garai T, Santra U. 2023. A possibility-based multi-criteria decision-making approach for artificial recharge structure selection using pentagonal fuzzy numbers. Decision Analytics Journal, 9: 100365. DOI：10.1016/j.dajour.2023.100365.

Diakoulaki D, Mavrotas G, Papayannakis L. 1995. Determining objective weights in multiple criteria problems: The critic method. Computers & Operations Research, 22: 763−770. DOI：10.1016/0305-0548(94)00059-H.

Dörr F, Bauer J, Tran HV, et al. 2023. Vietnam's mekong delta- land subsidence due to groundwater over-exploitation. Wasserwirtschaft, 113: 52−56. DOI：10.1007/s35147-023-1922-3.

Dubey RS, Chattopadhyay PB, Pal U. 2024. Identifying potential artificial recharge zone in an arid craton. Groundwater for Sustainable Development, 27: 101338. DOI：10.1016/j.gsd.2024.101338.

Fan ZR, Wang YY, OYang W, et al. 2023. Artificial groundwater recharge potential and recharge mode in the Shichuan River valley area. South-to-North Water Transfers and Water Science & Technology, 491−500. (in Chinese) DOI：10.13476/j.cnki.nsbdqk.2023.0049.

Gao W. 2013. Effect of long-distance raw water pipeline on typical water quality indicators. China Water & Wastewater, 29: 4. (in Chinese) DOI：10.19853/j.zgjsps.1000-4602.2013.19.016.

Hammouri N, Al-Amoush H, Al-Raggad M, et al. 2014. Groundwater recharge zones mapping using GIS: A case study in Southern part of Jordan Valley, Jordan. Arabian Journal of Geosciences, 7: 2815−2829. DOI：10.1007/

s12517-013-0995-1.

Heng T, Chen GH. 2013. Application of hierarchical equations of motion (HEOM) to time dependent quantum transport at zero and finite temperatures. The European Physical Journal B, 86: 411. DOI：10.1140/epjb/e2013-40333-7.

Houle ES, Livneh B, Kasprzyk JR. 2017. Exploring snow model parameter sensitivity using Sobol' variance decomposition. Environmental Modelling & Software, 89: 144−158. DOI：10.1016/j.envsoft.2016.11.024.

Jamali MY, Namous M, SoumiaAmir. 2020. Impact of overexploitation of groundwater along the irrigated perimeter of Tadla, Oum Errabia Basin, Morocco. Desalination and Water Treatment, 195: 201−212. DOI：10.5004/dwt.2020.25877.

Jena S, Panda RK, Ramadas M, et al. 2020. Delineation of groundwater storage and recharge potential zones using RS-GIS-AHP: Application in arable land expansion. Remote Sensing Applications: Society and Environment, 19: 100354. DOI：10.1016/j.rsase.2020.100354.

Kadiri M, Zarhloule Y, Barkaoui A-e, et al. 2023. Identification of potential artificial groundwater recharge sites using GIS and the analytical hierarchy process: Case study of Tamellalt plain, Morocco. Hydrogeology Journal, 31: 1813−1828. DOI：10.1007/s10040-023-02701-x.

Lian H, Sun Z, Xu C, et al. 2023. Groundwater level dynamic simulation and soil salinization prediction of the closed hydrogeological unit in the arid irrigation area. Journal of Hydroinformatics, 25: 815−834. DOI：10.2166/hydro.2023.142.

Maqbool S, Singh V, Patley MK, et al. 2024. Evaluation of groundwater quality potential zones using AHP and WIOA models in Shopian District, Jammu and Kashmir, India: A GIS. Journal of Hazardous Materials Advances, 16: 100488. DOI：10.1016/j.hazadv.2024.100488.

Martelli G, Granati C, Paiero G, et al. 2014. Artificial recharge of phreatic aquifer in the Mereto Di Tomba Area (Upper Friuli Plain). Procedia Engineering (Netherlands), 89: 1241−1248. DOI：10.1016/j.proeng.2014.11.427.

Mengstie L, Nebere A, Jothimani M, et al. 2024. Landslide susceptibility assessment in Addi Arkay, Ethiopia using GIS, remote sensing, and AHP. Quaternary Science Advances, 15: 100217. DOI：10.1016/j.qsa.2024.100217.

Mishra U, Mohapatra AK, Mandal A, et al. 2023. Identification of potential artificial groundwater recharge sites in an alluvial setting: A coupled electrical resistivity tomography and sediment characterization study. Groundwater for Sustainable Development, 20: 100875. DOI：10.1016/j.gsd.2022.100875.

Mogaji KA, Omosuyi GO, Adelusi AO, et al. 2016. Application of GIS-based evidential belief function model to regional groundwater recharge potential zones Mapping in Hardrock Geologic Terrain. Environmental Processes, 3: 93−123. DOI：10.1007/s40710-016-0126-6.

Rachdi L, Abdelkrim B, Atoui M, et al. 2024. Assessment of groundwater potential recharge areas using advanced decision models and spatial data: Applied to Sbeitla aquifer system, central Tunisia. Groundwater for Sustainable Development, 27: 101316. DOI：10.1016/j.gsd.2024.101316.

Raja Shekar P, Mathew A. 2023. Assessing groundwater potential zones and artificial recharge sites in the monsoon-fed Murredu river basin, India: An integrated approach using GIS, AHP, and Fuzzy-AHP. Groundwater for Sustainable Development, 23: 100994. DOI：10.1016/j.gsd.2023.100994.

Rani M, Joshi H, Kumar K, et al. 2019. Development of recharge and conservation site suitability model for groundwater retrieval and evaluation of artificial recharge potential in a complex hydro-geological spring-fed river basin. Arabian Journal of Geosciences, 12: 589. DOI：10.1007/s12517-019-4784-3.

Sethuraman S, Alshahrani HM, Tamizhselvi A, et al. 2024. Assessment of coastal vulnerability using AHP and machine learning techniques. Journal of South American Earth Sciences, 147: 105107. DOI：10.1016/j.jsames.2024.105107.

Saaty RW. 1987a. The analytic hierarchy process—what it is and how it is used. Mathematical Modelling, 9: 161−176. DOI：10.1016/0270-

0255(87)90473-8.

Saaty TL. 1983. Introduction to a modeling of social decision processes. Mathematics and Computers in Simulation, 25: 105−107. DOI：10.1016/0378-4754(83)90072-1.

Saaty TL. 1987b. How to handle dependence with the analytic hierarchy process. Mathematical Modelling, 9: 369−376. DOI：10.1016/0270-0255(87)90494-5.

Sahaar SA, Niemann JD. 2020. Impact of regional characteristics on the estimation of root-zone soil moisture from the evaporative index or evaporative fraction. Agricultural Water Management, 238: 106225. DOI：10.1016/j.agwat.2020.106225.

Salehi Shafa N, Babazadeh H, Aghayari F, et al. 2023. Optimal utilization of groundwater resources and artificial recharge system of Shahriar plain aquifer, Iran. Physics and Chemistry of the Earth, Parts A/B/C, 129: 103358. DOI：10.1016/j.pce.2023.103358.

Sandoval JA, Tiburan CL. 2019. Identification of potential artificial groundwater recharge sites in Mount Makiling Forest Reserve, Philippines using GIS and Analytical Hierarchy Process. Applied Geography, 105: 73−85. DOI：10.1016/j.apgeog.2019.01.010.

Shahkarami N. 2024. Temporal analysis of land subsidence and groundwater depletion using the DInSAR and Kriging methods: A case study and insights. Journal of Hydrologic Engineering, 29(3): 04024011. DOI：10.1061/JHYEFF.HEENG-6130.

Song X, Zhang J, Zhan C, et al. 2015. Global sensitivity analysis in hydrological modeling: Review of concepts, methods, theoretical framework, and applications. Journal of Hydrology, 523: 739−757. DOI：10.1016/j.jhydrol.2015.02.013.

Subba Rao N, Gugulothu S, Das R. 2022. Deciphering artificial groundwater recharge suitability zones in the agricultural area of a river basin in Andhra Pradesh, India using geospatial techniques and analytical hierarchical process method. Catena, 212: 106085. DOI：10.1016/j.catena.2022.106085.

Wang HY, Song CQ, Wang JF, et al. 2024. A raster-based spatial clustering method with robustness to spatial outliers. Scientific Reports, 14: 4103. DOI：10.1038/s41598-024-53066-4.

Wang YZ, Ye NJ. 2008. Farmland drainage problems in the Huaibei Plain, Anhui Province. China Rural Water and Hydropower, (2): 5–7, 13. Available on https://irrigate.whu.edu.cn/CN/Y2008/V0/I2/5 (in Chinese)

Wu SJ, Tetzlaff D, Yang XQ, et al. 2022. Identifying dominant processes in time and space: Time-varying spatial sensitivity analysis for a grid-based nitrate model. Water Resources Research, 58: e2021WR031149. DOI：10.1029/2021WR031149.

Xu YY, Lü HS, Yagci A, et al. 2024. Influence of groundwater on the propagation of meteorological drought to agricultural drought during crop growth periods: A case study in Huaibei Plain. Agricultural Water Management, 305: 109122. DOI：10.1016/j.agwat.2024.109122.

Zhang YW. 2020. Evaluation of groundwater artificial recharge suitability in plain area of Daqing River Basin based on GIS - EWM. M. S. thesis, Jilin University.

Zaidi FK, Nazzal Y, Ahmed I, et al. 2015. Identification of potential artificial groundwater recharge zones in Northwestern Saudi Arabia using GIS and Boolean logic. Journal of African Earth Sciences, 111: 156−169. DOI：10.1016/j.jafrearsci.2015.07.008.

Zhang H, Xu YX, Kanyerere T. 2020. A review of the managed aquifer recharge: Historical development, current situation and perspectives. Physics and Chemistry of the Earth, Parts A/B/C, 118−119: 102887. DOI：10.1016/j.pce.2020.102887.

Zhang YF, Wang YF, L, iu LX. 2001. Function mechanism between the drought and waterlogging disaster and the Soil-structure of the Shajiang soil in Huaibei Plain. Progress in Geography, 20: 169−176. (in Chinese) DOI：10.11820/dlkxjz.2001.02.010.